XXIV FIG International Congress 2010
11-16 April 2010
Sydney, Australia

Monitoring of Bridge Deformation with InSAR: An Experimental Study

Lei Zhang[1], Xiaoli Ding[1] and Zhong Lu[2]

1 *Department of Land Surveying and Geo-Informatics, The Hong Kong Polytechnic University, Hung Hom, KLN, Hong Kong*

2 *U.S. Geological Survey, Vancouver, Washington, USA*

The Hong Kong Polytechnic University 香港理工大學

Department of Land Surveying and Geo-Informatics 測量與地理資訊學系

USGS science for a changing world

The Donghai Bridge

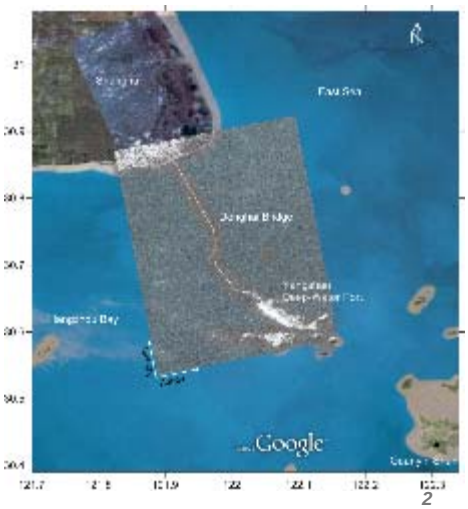

2

Location: North of Hangzhou Bay
Length: 32.5km
Width: 31.5m

Linking mainland Shanghai with Yangshan deep-water port

Operation since 2005

Cable stayed section with a span of 420m

Method – TCP-InSAR (1)

Multi-temporal InSAR: Temporarily Coherent Point InSAR (TCPInSAR)

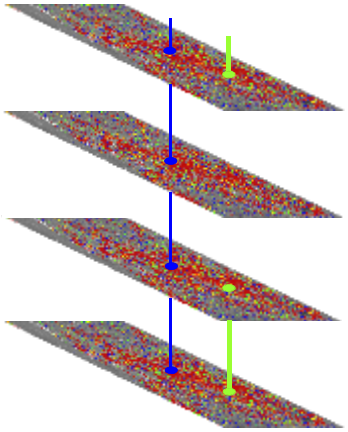

- TCP identification
- Co-registration
- Point networking
- Least squares based solution

3

Method – TCP-InSAR (2)

Advantages:

- Easy to implement
- Able to get a solution based on very small number of SAR images

- [1] Zhang, L., Ding, X.L., and Lu, Z. (2009), Least squares solution of small sample multiple master PSI systems, Fringe2009, Italy.
- [2] Zhang, L., Ding, X.L., Lu, Z., and Feng, G. C. (2009), Ground settlement monitoring from temporarily persistent scatterers between two SAR acquisitions, 2009 Joint Urban Remote Sensing Event, Shanghai.
- [3] Zhang, L., Ding, X.L., and Lu, Z., Ground settlement monitoring from temporarily coherent points between two SAR acquisitions, ***ISPRS Journal of Photogrammetry and Remote Sensing*** (2nd review).
- [4] Zhang, L., Ding, X.L., and Lu, Z., Modeling the PSInSAR time-series without phase unwrapping, ***IEEE Transactions on Geoscience and Remote Sensing*** (under revision).

4

SAR Data and TCP Identification (1)

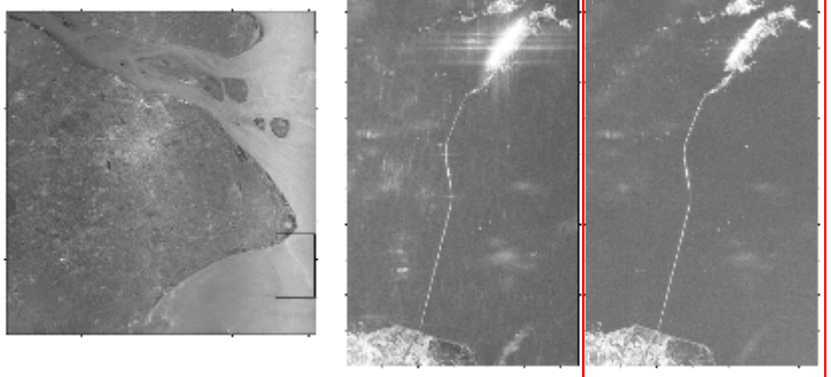

Envisat/ASAR | ALOS/PALSAR-HH polarization | ALOS/PALSAR-HV polarization

5

SAR Data and TCP Identification (2)

4 ALOS PALSAR images acquired on the following dates:

20090112
20090227
20090414
20090715

SAR Data and TCP Identification (3)

3 interferograms:

Master	Slave	B_perp(m)	B_temp(day)
20090112	20090227	115	46
20090112	20090414	822	92
20090112	20090715	959	184

SAR Data and TCP Identification (4)

- **Temporarily Coherent Point (TCP) selection**

Stable targets have consistent offset values

- **Offset vector map over Shanghai area**

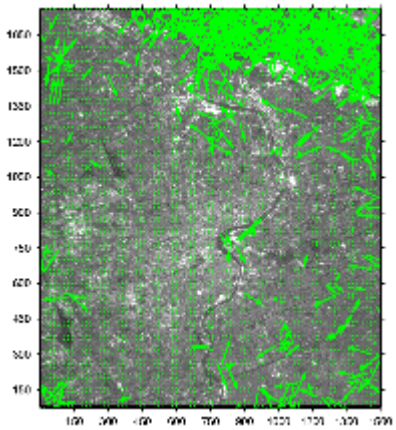

Patch size: 16*16

Ovs. factor: 2

Res. : 20p*100p

Ini. offset has been removed!

Statistics of offsets

8

SAR Data and TCP Identification (5)

- **Characteristics of offsets at TCP**
  - After removing initial offsets, offsets at TCP appear to be consistent at least in pixel level in spatial domain
  - Offset estimation at TCP are not sensitive to the window size and oversampling factor.
- **Implementation**

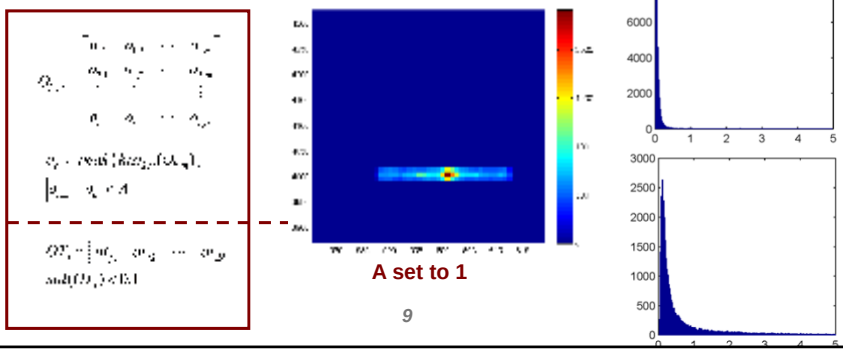

9

SAR Data and TCP Identification (6)

- **Advantages**
  - The amplitude data need not to be calibrated
  - No assumptions on the temporal behavior of the considered pixel
  - No parameters need to be set based on experience
- **TCP along Donghai Bridge**

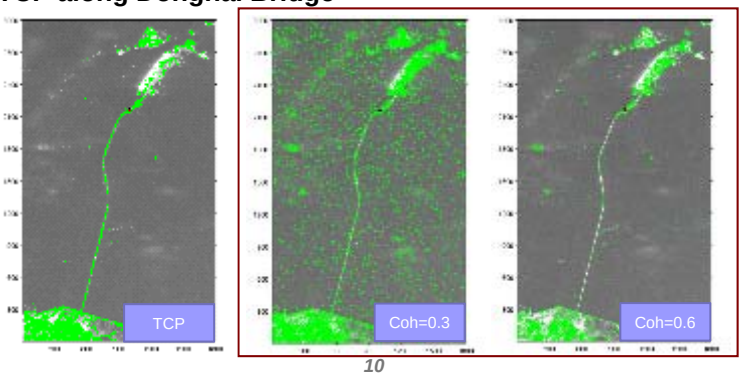

10

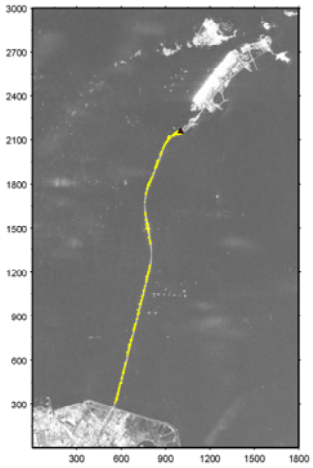

517 points on the bridge in total

Coregistration(1)

- **Using the polynomial determined only from offsets on TCP**

Table 2. The polynomial determined from Cut-off-Go

		a	b	c	d	e	f
Range	Conventional						
	TCP method						
Azimuth	Conventional						
	TCP method						

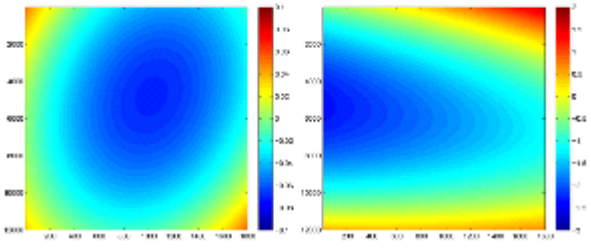

Range difference **Azimuth difference**

Coregistration(2)

The impacts of coregistration error on interferometric phase (1) and coherence (2)

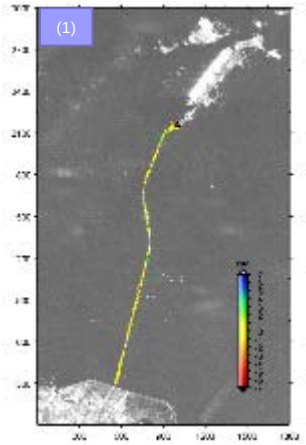

Mean (abs(ph_diff)): 1.2 rad

Std(abs(ph_diff)): : 1.5 rad

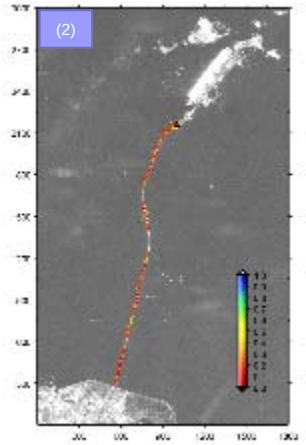

Mean: 0.2; Std: 0.13

13

TCP Networking

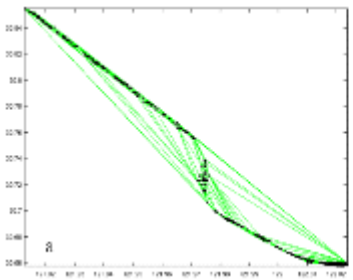

Global triangulation

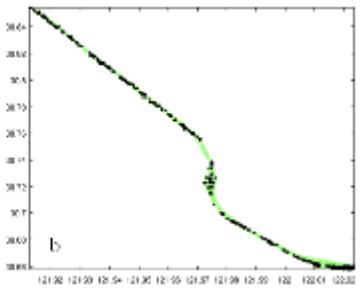

Local triangulation

Local triangulation (517 points along the bridge)

- To increase the density of point pairs (i.e., arcs)
- No need of detecting and removing long arcs

without much increase of computation complexity

14

TCP Least Squares Based Model (1)

- **Multiple master interferogram stacking**

J : images

I : interferograms with short baselines

$$\phi_{i,x} = \phi_{i,x-1,x} + \phi_{x-1,x} \approx \phi_{i,i+1,x} + \phi_{i+1,x} + \phi_{i,i+1,x}$$

$$\phi_{i+1,x} \approx \frac{4\pi}{\lambda}\Delta r_{i,x} \approx \frac{4\pi}{\lambda}\sum_{j=i+1}^{x-1}(t_j - t_{j-1})V_j + \beta_i V$$

$$\phi_{i,i+1,x} \approx \frac{4\pi}{\lambda}\frac{B^{\perp}_{i,i+1}}{r_{i,x}\sin\theta^{i}_{i,x}}\Delta h_{i,x} \approx \alpha_{i,x}\Delta h_{i,x}$$

$$A\phi^{i}_{i,i+1,x} = \alpha^{i}_{i,x}\Delta h_{i,x} - \beta_i \Delta V - w^{i}_{i,i+1,x}$$

$$w^{i}_{i,i+1,x} \approx \Delta\phi^{i}_{i,i+1,i,i+1} + \Delta\phi^{i}_{i+1,i+1,x} + \Delta\phi^{i}_{i,i+1,x}$$

For the arc having no phase ambiguities, we have

$$A\Phi = A\begin{bmatrix}\Delta h_{1,2,\ldots,x-1,x}\\ \Delta V\end{bmatrix} - W$$

$$A\Phi = \left|A\phi^{1}_{1,2,\ldots,x-1,x} \quad A\phi^{2}_{1,2,\ldots,x-1,x} \quad \cdots \quad A\phi^{I}_{1,2,\ldots,x-1,x}\right|^{T}$$

$$A = [\alpha \quad \beta]$$

$$\alpha = \left[\alpha^{1}_{1,x} \quad \alpha^{2}_{1,x} \quad \cdots \quad \alpha^{I}_{1,x}\right]^{T}$$

$$\beta = \left[\beta_1 \quad \beta_2 \quad \cdots \quad \beta_I\right]^{T}$$

$$W = \left[w^{1}_{1,2,\ldots,x} \quad w^{2}_{1,2,\ldots,x} \quad \cdots \quad w^{I}_{1,2,\ldots,x}\right]$$

15

TCP Least Squares Based Model (2)

- **Least squares solution**

The functional and stochastic models of observations

$$E\{A\Phi\} = A\begin{bmatrix}\Delta h_{1,2,\ldots,x-1,x}\\ \Delta V\end{bmatrix} = A\Phi - W$$

$$D\{\Delta\Psi\} = Q^{ww}$$

$$Q^{-1} = 2Q^{-1}_{ww} = 2DQ_{xx}D^{T}$$

$$P^{ww} = (Q^{ww})^{-1}$$

Least squares solution

$$\begin{bmatrix}\Delta h_{1,2,\ldots,x-1,x}\\ \Delta V\end{bmatrix} = \left(A^{T}P^{ww}A\right)^{-1}A^{T}P^{ww}A\Phi$$

$$\Delta\Psi = A\left(A^{T}P^{ww}A\right)^{-1}A^{T}P^{ww}\Delta\Phi$$

$$v = A\Phi - A\left(A^{T}P^{ww}A\right)^{-1}A^{T}P^{ww}A\Phi$$

Covariance matrices

$$D\left\{\begin{bmatrix}\Delta h_{1,2,\ldots,x-1,x}\\ \Delta V\end{bmatrix}\right\} = Q_{xx} = \left(A^{T}P^{ww}A\right)^{-1}$$

$$D\{A\Phi\} = Q_{AA\Phi\Phi} = A\left(A^{T}P^{ww}A\right)^{-1}A^{T}$$

$$D\{v\} = Q_{vv} = Q_{ww} - A\left(A^{T}P^{ww}A\right)^{-1}A^{T}$$

16

TCP Least Squares Based Model (3)

- **Outlier detection**

$$Max(v_i^j) > c_0\sqrt{Max((Q^{vv})_{ii})} + 2_0\sqrt{Max((Q_{\hat{l}\hat{l}})_{ii})}$$

- **Final solution**

A. One reference point

$$L = L^0 + S_1 R_1$$

$$X = \begin{bmatrix} x_1 & x_2 & \cdots & x_{s-1} & x_{s+1} & \cdots & x_u \end{bmatrix}$$

$$LL = ULX$$

$$Y = \left(UL^T PLU\right)^{-1} UL^T P$$

B. Multiple reference points

$$\begin{bmatrix} C & X_1 & W_1 \\ \cdots & \cdots & \cdots \\ A & \cdots & \cdots \end{bmatrix} \quad 0$$

$$X = \begin{bmatrix} N_{aa}^{-1} & N_{aa}^{-1}C^T N_{rr}^{-1}(CN_{aa}^{-1}) \end{bmatrix} \begin{bmatrix} \cdots \\ N_{aa}^{-1}C^T N_{rr}^{-1} \end{bmatrix} W_1$$

where

$$N_{aa} = UU^T PUU, Z = UU^T PLL, N_{rr} = CN_{aa}C^T$$

TCP Least Squares Based Model (4)

- **Advantages**

By focusing on arcs without phase ambiguities

- No need of phase unwrapping

- Solution efficiency is improved greatly

Results (1)

- **Validation**

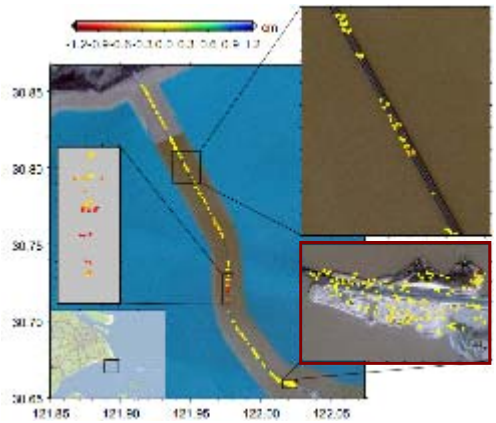

Assuming that no deformation occurred on the island, the RMS of deformation rates of the points on the island is 1.2 mm/y.

Master	Slave	B_perp(m)	B_temp(day)
20090112	20090227	115	46
20090112	20090414	822	92
20090112	20090715	959	184

19

Results (2)

- **Analysis**

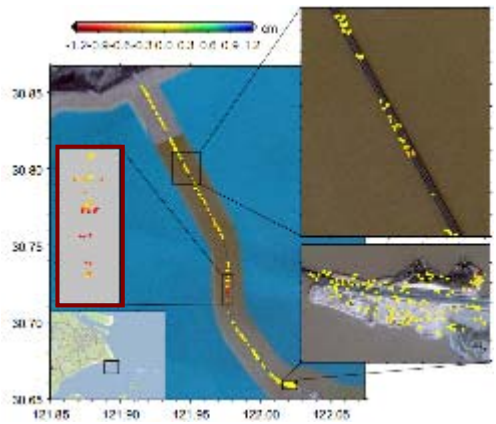

Largest deformation occurred on the cable-stayed bridge, up to 1.2cm from January 2009 to July 2009

The PALSAR data used were acquired at 10:23 pm local time in January, February, April and July respectively and the mean night-time temperature in those months was 1℃, 1℃, 10℃ and 23℃.

Temperature changes

20

Conclusions

- The proposed method can identify enough coherent points on the bridge and can estimate the deformation rate from a small set of SAR interfergrams.
- The results from TCP along the bridge have shown that notable deformation occurred on the cable-stayed section which may be related to the temperature change.

21

l.zhang@polyu.edu.hk
lsxlding@polyu.edu.hk
lu@usgs.gov

22